RSC Advances

PAPER

Cite this: *RSC Adv.*, 2018, **8**, 31889

A novel off-on fluorescent chemosensor for Al^{3+} derived from a 4,5-diazafluorene Schiff base derivative†

Hui Li, *[ab] Jianzhi Wang,[a] ShuJiang Zhang,[b] ChenLiang Gong [b] and Feng Wang [a]

Received 20th June 2018
Accepted 21st August 2018

DOI: 10.1039/c8ra05280h

rsc.li/rsc-advances

The performance of a chemosensor is closely related to its structure. A new Schiff bass (**DFSB**) based on 4,5-diazafluorene units has been synthesized in this work. The interaction of **DFSB** with different metal ions has been studied using UV-vis absorption spectra and fluorescent spectra. The results show that **DFSB** is a highly selective and sensitive probe for Al^{3+} ions over other commonly coexisting metal ions in ethanol. A very obvious fluorescence enhancement effect was observed, and a turn-on ratio over 1312-fold was triggered with the addition of 10 equiv. of Al^{3+} ions. What is more, such fluorescent responses could be detected by the naked eye under a UV-lamp. The lowest detection limit for Al^{3+} was determined as 3.7×10^{-8} M. The complex solution (**DFSB**–Al^{3+}) exhibited reversibility with EDTA. These results may be caused by the unique molecular structure.

1 Introduction

Al^{3+} ions existing in natural waters and most plants can enter the human body through foods and water.[1] The normal concentration range for aluminum ions in biological systems is narrow, with both deficiency and excess causing many pathological states, such as Alzheimer's disease, Parkinson's disease, chronic renal failure, bone softening and smoking related diseases.[2–6] Since there is a close association between Al^{3+} and human health, developing fluorescent chemosensors with high selectivity and sensitivity for detecting trace amounts of Al^{3+} has attracted increasing attention.

In recent years, chemosensors have attracted significant interest because of their high sensitivity, selectivity, rapid response[7,8] and simplicity[9] and have been widely used in many fields such as public health,[10–12] metal ion detection,[13–16] environmental monitoring[17–19] and disease diagnosis. Incorporation of specific functional structure unit into the fluorescent chemosensors leads to advanced functional materials that exhibit certain advantageous properties, such as highly selective and sensitive sensor for analysis.[20] In addition, fluorescent sensors based on a large group of structurally different fluorophores, including coumarin,[21,22] 8-hydroxyquinoline,[23] naphthalene,[24] rhodamine,[25–27] pyrrolidine,[28] calixarene,[29] hydroxyflavone,[30,31] thiazole,[32] oxazoline and imidazoline[33] have been developed. These sensors have sufficiently high selectivity. However, for many of them, the fluorescent response and detection limit of a determined cation is not sufficient. For example, the sensor based on julolidine shows only 7.8-fold fluorescence buildup by reaction with Zn^{2+} ions.[34] Therefore, the aim of determining simple structure and obtaining fluorescent chelating ligands capable of acting both as a selective chemical reagent and an "off–on" fluorescent cation sensor is very relevant.

4,5-Diazafluorene is one of the most powerful building blocks for creating multifunctional structures. These compounds have similarities to 2,2′-bipyridyl and 1,10-phenanthroline derivatives.[35] Furthermore, these compounds can form various complexes by coordination to metal ions such as Fe^{3+},[36] Cu^{2+},[37,38] Cd^{2+},[39] Eu^{3+},[40] and Ru^{2+}.[41,42] The 4,5-diazafluorene has been chosen as an ideal structure of a fluorescent chemosensor due to its large π-system and bidentate coordination ability with various metal ions. Some Ru(II) polypyridyl complexes containing 4,5-diazafluorene units has been employed as fluorescent probes for metal ions.[43–45] However, the fluorescent chemosensors based on the binding ability of 4,5-diazafluorene units to metal ions is rarely.[46,47]

Herein, we report the synthesis and characterization of a Schiff base ligand (**DFSB**) obtained by condensing 9,9-bis(4-aminophenyl)-4,5-diazafluorene with salicylaldehyde. The Al^{3+} recognition ability were investigated. The free chemosensor **DFSB** shows weak fluorescence emission. Upon binding of Al^{3+}, a significant fluorescence enhancement over 1314-fold is achieved in ethanol.

[a]*Key Laboratory for Green Chemical Process of Ministry of Education, School of Chemical Engineering and Pharmacy, Wuhan Institute of Technology, Wuhan 430205, P. R. China. E-mail: sodium2008@wit.edu.cn*

[b]*College of Chemistry and Chemical Engineering, Lanzhou University, Lanzhou 730000, P. R. China*

† Electronic supplementary information (ESI) available. See DOI: 10.1039/c8ra05280h

2 Experiment

2.1 Materials and instrumentation

The reactants 4,5-diazafluoren-9-one (**1**)[48] was prepared according to the literature. Aniline (Tianjin Guangfu) was purified by distillation prior to use. All organic solvents were of analytical reagent grade. Nitrate and chloride salt of all cations used were of high purity and used without any purification.

The stock solution for **DFSB** (3 mM) were prepared in DMSO, stock solution for nitrate and chloride salt of different metals of Ag^{+}, Al^{3+}, Ba^{2+}, Ca^{2+}, Cd^{2+}, Co^{2+}, Cr^{3+}, Cu^{2+}, Fe^{2+}, Fe^{3+}, Hg^{2+}, K^{+}, Li^{+}, Mg^{2+}, Mn^{2+}, Na^{+}, Ni^{2+}, Sr^{2+}, Pb^{2+} and Zn^{2+} were prepared by dissolving the salts in deionized water to the final concentrations of 1.0 mM. The absorption and fluorescence titrations were performed on 10.0 μM solutions of **DFSB** in ethanol and the aliquots of freshly prepared standard aqueous solutions of metal ions were added to record the absorption and fluorescence spectra. Each spectrum was recorded 40 min after Al^{3+} addition.

The ^{1}H NMR and ^{13}C NMR spectra were measured on a JEOL EX-400 spectrometer using DMSO-d_6 as solvent and tetramethylsilane as the internal reference. UV-vis spectra were examined on a Lambda 35 spectrophotometer and fluorescent recorded on a LS-55 spectrofluorophotometer with excitation slit at 15.0 nm and emission at 7.0 nm.

2.1.1 Binding constant calculation. The binding constants of the inclusion complex were obtained from the fluorescence titration data. According to the Benesi–Hildebrand method, the equation for a 1 : 1 host : guest complex is given below:

$$\log\frac{F - F_{\min}}{F_{\max} - F} = \log[\mathrm{M}] - \log K_{\mathrm{d}}$$

In this equation K_d is the dissociation constant and different fluorescence emission intensity F_{min}, F and F_{max} are the find out at $\lambda_{max} = 475$ nm, for the complex at initial, interval, and the final state of complex. Concentrations of metal represent by M and association constant (K_a) was determined by $K_a = 1/K_d$.

2.1.2 Determination of detection limit. The detection limits (DLs) of **DFSB** for Al^{3+} were calculated using the following equation:

$$\mathrm{DL} = \frac{3\sigma}{S}$$

where σ is the standard deviation of the blank measurement, which is 0.077 here, and S is the slope between the emission intensity *vs.* the concentration of aluminium ion.

2.2 Monomer synthesis

2.2.1 Synthesis of 9,9-bis(4-aminophenyl)-4,5-diazafluorene (2). 9,9-bis(4-aminophenyl)-4,5-diazafluorene was synthesized by accordingly to describe the method in Scheme 1. Methanesulfonic acid (4.04 g, 41 mmol) was slowly added to the aniline (19.56 g, 210 mmol) was placed in a 100 ml three-necked flask with magnetic stirring and a nitrogen inlet. Then, 4,5-diazafluoren-9-one (5.45 g, 30 mmol) was added. The mixture was the heated to 155 °C for 24 h under an atmosphere of nitrogen with continuous stirring. The solution was cooled below 80 °C followed by neutralization with a solution of 5% sodium hydroxide. The precipitate was filtered and washed with water and ethanol. The crude product was purified by recrystallization to give a white powder (4.04 g, yield: 59%), mp: >300 °C.

IR (KBr, cm^{-1}): 3454 (NH), 3331 (NH), 3066–3004 cm^{-1} (C–N), 1510 cm^{-1} (C=N); ^{1}H NMR (400 MHz, DMSO-d_6, δ, ppm, TMS, Fig. S1†): 5.03 (s, 2H, $-NH_2$), 6.42 (d, H^2, $J = 8.4$ Hz, 2H), 6.75 (d, H^3, $J = 8.4$ Hz, 2H), 7.35 (dd, H^8, $J = 4.8$, 4.8 Hz), 7.84 (dd, H^7, $J = 1.6$, 1.6 Hz, 2H), 8.62 (dd, H^9, $J = 1.6$, 1.6 Hz, 2H); ^{13}C NMR (100 MHz, DMSO-d_6, δ, ppm, TMS, Fig. S1†): 59.8 (C^5),

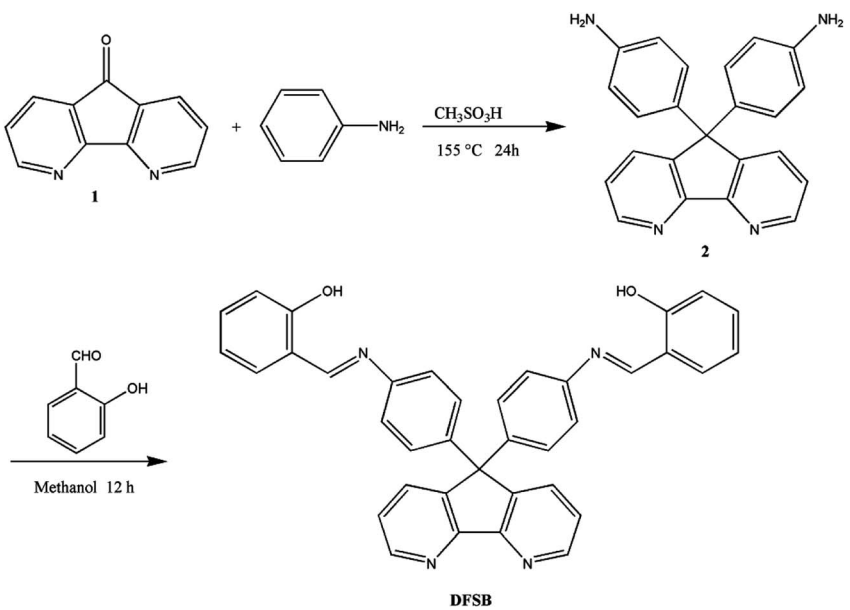

Scheme 1 Synthesis of the Schiff base DFSB.

114.1 (C^2), 123.9 (C^8), 128.5 (C^3), 131.0 (C^6), 134.2 (C^7), 147.5 (C^4), 148.0 (C^1), 149.7 (C^9), 157.1 (C^{10}).

2.2.2 Synthesis of 4,5-diazafluorene Schiff bases (DFSB). 9,9-bis(4-aminophenyl)-4,5-diazafluorene (0.175 g, 0.5 mmol) was placed into a 100 ml round-bottom flask which was fitted with condenser, thermometer and magnetic stirrer. Methanol (50 ml) was added into the flask and reaction mixture was heated up to 80 °C. A solution of salicylaldehyde (0.183 g, 1.5 mol) in 20 ml methanol was added into the flask. Reactions were maintained for 12 h under reflux. The precipitated monomers was filtered hot and dried in a vacuum desiccator. (0.24 g, yield: 85.7%). ^{1}H NMR (DMSO-d_6, δ, ppm, TMS, Fig. S2†): 12.95 (s, –OH), 8.91 (s, H^7, J = 1.2 Hz, 2H), 8.74 (dt, H^{16}, J = 4.8, 1.2 Hz, 2H), 8.12–8.04 (dt, H^{14}, J = 7.8, 1.4 Hz, 2H), 7.63 (dd, H^5, J = 7.8, 1.4 Hz, 2H), 7.48 (m, H^3, 2H), 7.41 (tt, H^{15}, J = 3.1, 2.4 Hz, 2H), 7.35 (dd, H^9, J = 8.6, 1.3 Hz, 4H), 7.25 (dd, H^{10}, J = 8.5, 1.2 Hz, 4H), 7.00–6.92 (m, H^2 and H,[4] 4H). ^{13}C NMR (DMSO-d_6, δ, ppm, TMS, Fig. S2†): 164.18 (C^1), 160.78 (C^7), 157.33 (C^{17}), 150.66 (C^8), 147.89 (C^{16}), 145.83 (C^{11}), 142.58 (C^{14}), 134.59 (C^3), 133.90 (C^{13}), 133.05 (C^5), 129.16 (C^{10}), 124.48 (C^9), 122.24 (C^4), 119.83 (C^{15}), 119.67 (C^6), 117.12 (C^2), 60.83 (C^{12}).

3 Result and discussion

3.1 Absorption spectra study of receptor DFSB

As seen in Fig. 1, the absorption spectrum of receptor **DFSB** exhibited four absorbance peaks. The intense absorption band in high energy region at 233 nm and a small hump at 258 nm was assigned as the absorption overlap of ligand-to-ligand-charge-transfer (LLCT) transitions,[49] Also, a broad band at 320 to 350 nm could be assigned to $\pi \rightarrow \pi^*$ transition of the C=N group from 4,5-diazafluorene moiety.[50] Upon addition of Al^{3+} ions, a significant change is observed in the UV-vis absorption spectra of **DFSB**, the absorption band of **DFSB** at 258 nm decreased with concomitant evolution of a new small hump at 251 nm; meanwhile, the broad band at 320 to 350 nm decreased with concomitant evolution of a new broad peak at 307 nm are assigned as MLCT absorptions. Clear isosbestic points at 241 nm, 263 nm and 380 nm are noticeable, which indicates the formation of only one active **DFSB**–Al^{3+} complex (Fig. 2). In order to further validate the stoichiometry of the receptor **DFSB** and Al^{3+}, Job's plot was carried out. The concentration dependent studies further confirmed the formation of 1 : 1 coordination complex between Al^{3+} and **DFSB** (Fig. S3†). Thus, the presumed binding mode of **DFSB**–Al^{3+} complex was given in the Fig. 2.

3.2 Fluorescence study of Al^{3+}

The fluorescence behavior of **DFSB** is canvassed upon the addition of various metal ions in ethanol. As shown in Fig. 3a, receptor **DFSB** alone displayed a very weak single fluorescence emission intensity at 475 nm (about 0.66) with an excitation 392 nm. Upon addition of other cations (Ag^+, Ba^{2+}, Ca^{2+}, Cd^{2+}, Co^{2+}, Cr^{3+}, Cu^{2+}, Fe^{2+}, Fe^{3+}, Hg^{2+}, K^+, Li^+, Mg^{2+}, Mn^{2+}, Na^+, Ni^{2+}, Sr^{2+}, Pb^{2+} and Zn^{2+}) no significant changes were observed except Mg^{2+} (about 51.5). But on addition of 10 equivalents of Al^{3+} ions, the fluorescence intensity of **DFSB** (10 μM) increased rapidly which shows the high selectivity of Al^{3+} ions. The fluorescence enhancement efficiency observed at 475 nm was 1312-fold

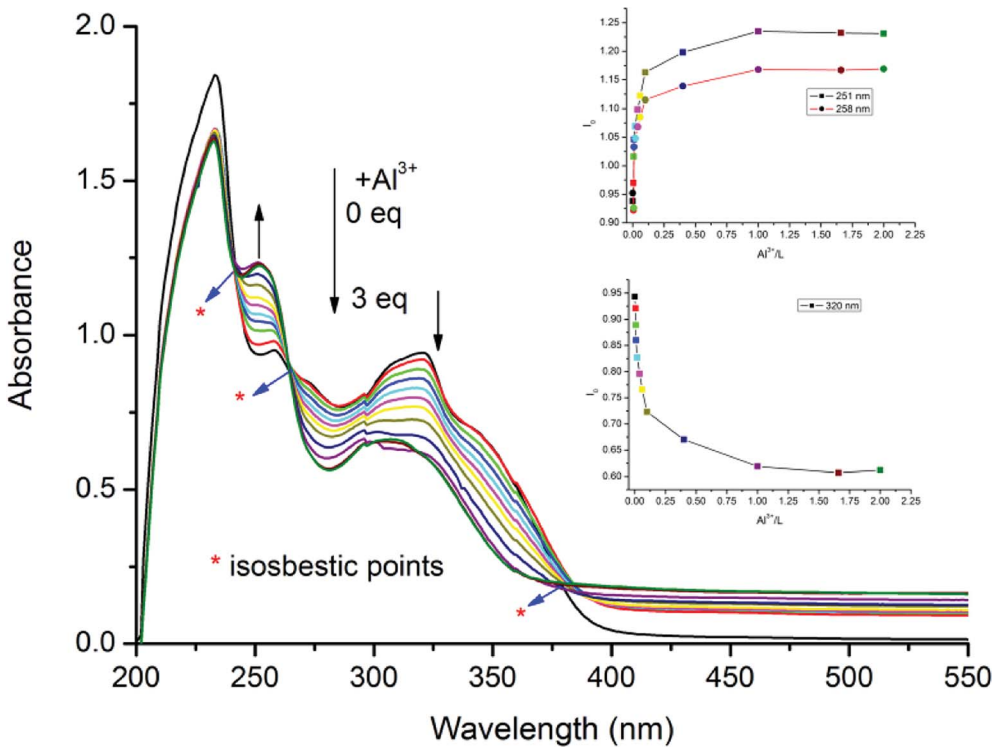

Fig. 1 UV-vis spectra of receptor **DFSB** (10 μM) in aqueous ethanol upon addition of increasing concentration of Al^{3+}. Inset: a plot of absorbance intensity as estimated by the peak height at 251 nm, 258 nm and 320 nm.

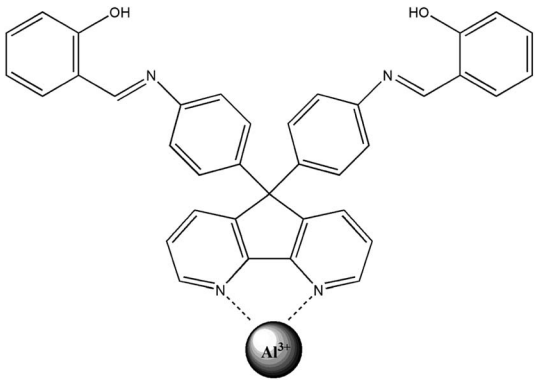

Fig. 2 The presumed binding mode of **DFSB**-Al^{3+} complex.

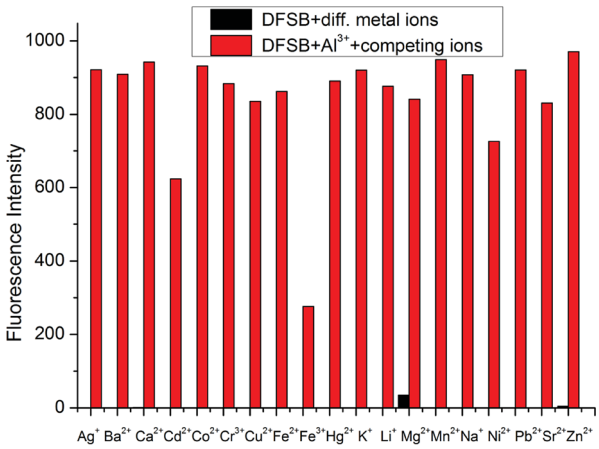

Fig. 4 Fluorescence response of receptor **DFSB** (10 μM) containing 10 equiv. of Al^{3+} to the selected metal ions (100 μM). The black bar represents emission intensity after adding 10 μM selected metal ions (Ag^{+}, Al^{3+}, Ba^{2+}, Ca^{2+}, Cd^{2+}, Co^{2+}, Cr^{3+}, Cu^{2+}, Fe^{2+}, Fe^{3+}, Hg^{2+}, K^{+}, Li^{+}, Mg^{2+}, Mn^{2+}, Na^{+}, Ni^{2+}, Pb^{2+}, Sr^{2+} and Zn^{2+}) in ethanol solution and red bar represent emission intensity after adding 10 μM of Al^{3+} in each of the above samples. Excitation wavelength (nm): 392.

greater than the control in the absence of Al^{3+} (Fig. 3b). In the absence of Al^{3+}, the extent of intramolecular charge transfer (ICT) in **DFSB** was sufficient enough to enhance its fluorescence. The chelation of **DFSB** with Al^{3+} not only enhanced the ICT effect in **DFSB** but also increased the rigidity of the molecular assembly resulting in a significant enhancement of the fluorescence intensity which is known as chelation-enhanced fluorescence (CHEF).[51] Based on the use of a UV lamp, the solution of receptor **DFSB** showed a dramatic color change from colorless to fluorescent blue in the presence of Al^{3+} ion, which could easily be detected by the naked-eye (Fig. 3c).

In order to establish the specific selectivity of **DFSB** to Al^{3+}, we performed the single and dual metal competitive analysis, as shown in Fig. 4. In a single metal system (black bars), all the metal ions (Ag^{+}, Ba^{2+}, Ca^{2+}, Cd^{2+}, Co^{2+}, Cr^{3+}, Cu^{2+}, Fe^{2+}, Fe^{3+}, Hg^{2+}, K^{+}, Li^{+}, Mg^{2+}, Mn^{2+}, Na^{+}, Ni^{2+}, Sr^{2+}, Pb^{2+} and Zn^{2+}) concentrations were kept as 100 μM towards **DFSB**. However, for the dual-metal (red bars) studies, two equal amounts of aqueous solutions of Al^{3+} and other metal ions (100 μM + 100 μM) were combined. From the bar diagram (Fig. 4), the PL intensity of the **DFSB** shows no obvious changes except for Fe^{3+}. Therefore, it was clear that other ions interference was negligibly small which were attributed to the unique structure of the **DFSB**. The unique selectivity of **DFSB** towards Al^{3+} could be interpreted in terms of the smaller ionic radii (0.5 Å) and higher charge density (r = 4.81) of the Al^{3+}. The smaller radii of the Al^{3+} permits a suitable coordination geometry of the chelating receptor **DFSB**

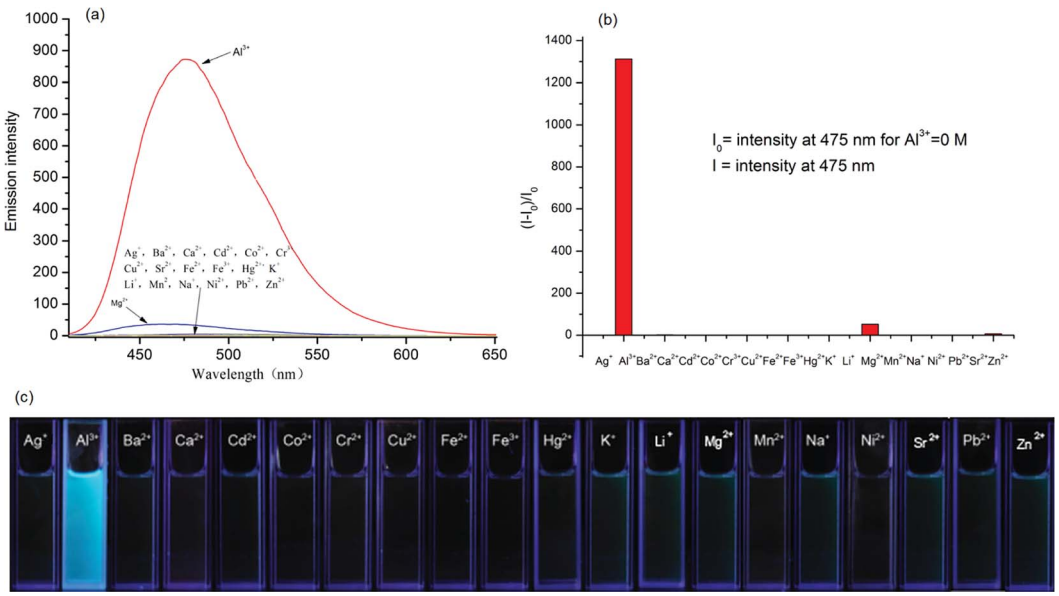

Fig. 3 (a) The fluorescence spectra of the **DFSB** (10 μM) in the presence of 10 equiv. of various metal ions in ethanol. Excitation wavelength (nm): 392. (b) Fluorescence emission response profiles for **DFSB** (10 μM) by adding various metal ions in ethanol. (c) Visual fluorescence emissions of sensor **DFSB** after addition of Ag^{+}, Al^{3+}, Ba^{2+}, Ca^{2+}, Cd^{2+}, Co^{2+}, Cr^{3+}, Cu^{2+}, Fe^{2+}, Fe^{3+}, Hg^{2+}, K^{+}, Li^{+}, Mg^{2+}, Mn^{2+}, Na^{+}, Ni^{2+}, Pb^{2+}, Sr^{2+} and Zn^{2+} (10 equiv.) in ethanol on excitation at 365 nm using UV lamp at room temperature.

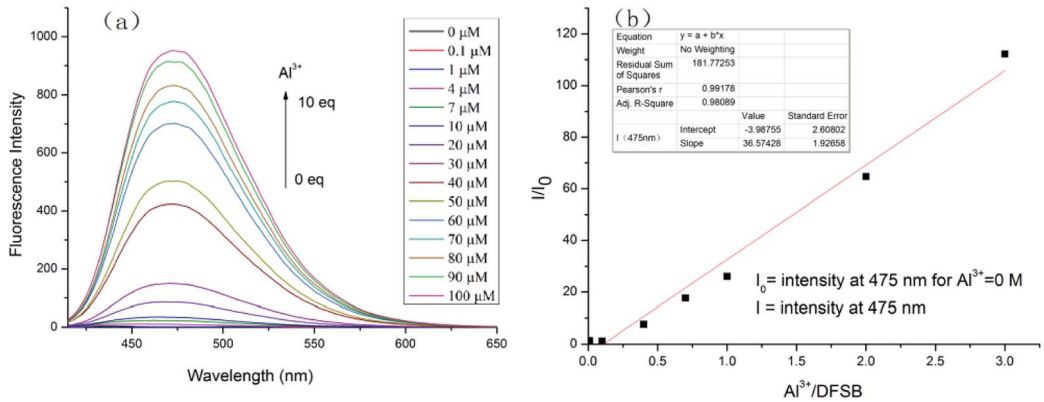

Fig. 5 (a) Fluorescence emission spectra of receptor **DFSB** (10 μM) in ethanol solution upon addition of increasing concentration of Al^{3+}. From bottom to top: [Al^{3+}] = (0, 0.1, 1, 4, 7, 10, 20, 30, 40, 50, 60, 70, 80, 90, 100 μM); (b) plot of fluorescence intensity at 475 nm *versus* the number of equivalents of Al^{3+} added. Excitation wavelength (nm): 392.

and the larger charge density allows a strong coordination ability between **DFSB** and Al^{3+}.[24]

Fluorescence titration experiments were carried out to investigate the complexation of Al^{3+} with the receptor **DFSB**. With an increasing concentration of Al^{3+}, the intensity of the maximum emission at 475 nm increased gradually (Fig. 5a). Using the calibration graph (Fig. 5b), it was possible to determine Al^{3+} in ethanol up to 30 μM. The calibration curve is linear with a correlation coefficient, $R^2 = 0.956$. From the fluorescent titration data, the detection limits was also measured to be 3.7×10^{-8} M (Fig. S4†) in ethanol. Moreover, the dissociation constants of **DFSB**–Al^{3+} was calculated to be 1.8×10^{9} M (Fig. S4†).

As shown in Fig. 6, the reversibility of sensor **DFSB** has been studied by the titration of EDTA with fluorescent probes (**DFSB** + Al^{3+}). The DFSB has very weak fluorescence emission intensity in ethanol. Upon adding Al^{3+} ions, the fluorescence intensity increases significantly. The fluorescence emission intensity returned to lower level for sensor **DFSB** after addition of EDTA. These results show that the addition of EDTA can completely destroyed the **DFSB**–Al^{3+} complex. This may be due to the coordination constant between EDTA–Al^{3+} is greater than **DFSB**–Al^{3+}.

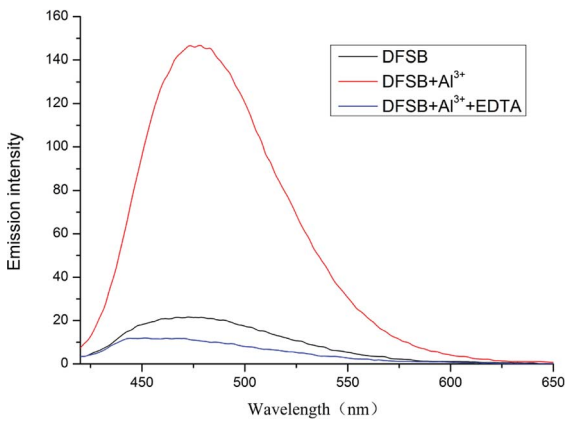

Fig. 6 Fluorescence emission spectra of receptor **DFSB** (10 μM) in the presence of Al^{3+} ions (30 μM) or EDTA (10 μM) in ethanol. Excitation wavelength (nm): 392.

4 Conclusion

In conclusion, A novel off-on fluorescent chemosensor for Al^{3+} derivated from 4,5-diazafluorene Schiff base derivative has been developed. The probe shows great fluorescence turn-on upon binding Al^{3+} and gives fluorescence enhancement by about 1312-fold at 475 nm. Moreover, the sensory system shows bright blue colour with Al^{3+} under a UV lamp, which can be easily identified by the naked eye. Thus, the reported sensor shows potential for detection of Al^{3+} using fluorescence spectroscopy.

Conflicts of interest

There are no conflicts to declare.

Acknowledgements

The authors are grateful for the research support from the National Natural Science Foundation of China [No. 21204033], China Postdoctoral Science Foundation (2017M612520), National Science Foundation of Hubei Province of China [2016CFB264, 2018CFB108] and the Program of Hubei Provincial Department of Education, China [Q20171507].

References

1 G. Berthon, *Coord. Chem. Rev.*, 1996, **149**, 241–280.
2 G. R. Legendre and A. C. Alfrey, *Clin. Chem.*, 1976, **22**, 53–56.
3 D. P. Perl and A. R. Brody, *Science*, 1980, **208**, 297–299.
4 D. P. Perl, D. C. Gajdusek, R. M. Garruto, R. T. Yanagihara and C. J. Gibbs, *Science*, 1982, **217**, 1053–1055.
5 M. H. Mashhadizadeh and H. Khani, *Anal. Methods*, 2010, **2**, 24–31.
6 L. Fan, J. Qin, T. Li, B. Wang and Z. Yang, *J. Lumin.*, 2014, **155**, 84–88.
7 V. K. Gupta, B. Sethi, R. A. Sharma, S. Agarwal and A. Bharti, *J. Mol. Liq.*, 2013, **177**, 114–118.
8 V. K. Gupta, L. P. Singh, R. Singh, N. Upadhyay, S. P. Kaur and B. Sethi, *J. Mol. Liq.*, 2012, **174**, 11–16.

9 E. V. Antina, N. A. Bumagina, A. I. V'Yugin and A. V. Solomonov, *Dyes Pigm.*, 2017, **136**, 368–381.
10 H. Karimi-Maleh, F. Tahernejad-Javazmi, N. Atar, M. L. Yola, V. K. Gupta and A. A. Ensafi, *Ind. Eng. Chem. Res.*, 2015, **54**, 3634–3639.
11 V. K. Gupta, A. Nayak, S. Agarwal and B. Singhal, *Comb. Chem. High Throughput Screening*, 2011, **14**, 284–302.
12 M. L. Yola, V. K. Gupta, T. Eren, A. E. Şen and N. Atar, *Electrochim. Acta*, 2014, **120**, 204–211.
13 V. K. Gupta, N. Mergu, L. K. Kumawat and A. K. Singh, *Sens. Actuators, B*, 2015, **207**, 216–223.
14 S. K. Srivastava, V. K. Gupta and S. Jain, *Anal. Chem.*, 1996, **68**, 1272–1275.
15 S. K. Srivastava, V. K. Gupta and S. Jain, *Analyst*, 1995, **120**, 495–498.
16 S. K. Srivastava, V. K. Gupta, M. K. Dwivedi and S. Jain, *Anal. Proc.*, 1995, **32**, 21–23.
17 V. K. Gupta, H. Karimi-Maleh and R. Sadegh, *Int. J. Electrochem. Sci.*, 2015, **10**, 303–316.
18 S. Karthikeyan, V. K. Gupta, R. Boopathy, A. Titus and G. Sekaran, *J. Mol. Liq.*, 2012, **173**, 153–163.
19 M. H. Dehghani, D. Sanaei, I. Ali and A. Bhatnagar, *J. Mol. Liq.*, 2016, **215**, 671–679.
20 V. K. Gupta, M. R. Ganjali, P. Norouzi, H. Khani, A. Nayak and S. Agarwal, *Crit. Rev. Anal. Chem.*, 2011, **41**, 282–313.
21 B. Sen, S. K. Sheet, R. Jamatia, A. K. Pal, R. Thounaojam, K. Aguan and S. Khatua, *Spectrochim. Acta, Part A*, 2017, **173**, 537–543.
22 J. Li, Y. Zeng, Q. Hu, X. Yu, J. Guo and Z. Pan, *Dalton Trans.*, 2012, **41**, 3623–3626.
23 N. Lashgari, A. Badiei and G. Mohammadi Ziarani, *J. Fluoresc.*, 2016, **26**, 1885–1894.
24 A. Sahana, A. Banerjee, S. Das, S. Lohar, D. Karak, B. Sarkar, S. K. Mukhopadhyay, A. K. Mukherjee and D. Das, *Org. Biomol. Chem.*, 2011, **9**, 5523–5529.
25 V. K. Gupta, N. Mergu and L. K. Kumawat, *Sens. Actuators, B*, 2016, **223**, 101–113.
26 V. K. Gupta, N. Mergu, L. K. Kumawat and A. K. Singh, *Talanta*, 2015, **144**, 80–89.
27 J. B. Li, H. Q. Hu, Y. Zeng, X. L. Yu and Z. Q. Pan, *Prog. Chem.*, 2012, **24**, 823–833.
28 Y. Wang, L. Xiong, F. Geng, F. Zhang and M. Xu, *Analyst*, 2011, **136**, 4809–4814.
29 A. B. Othman, J. W. Lee, Y.-D. Huh, R. Abidi, J. S. Kim and J. Vicens, *Tetrahedron*, 2007, **63**, 10793–10800.
30 R. S. Sathish, A. G. Raju, G. N. Rao and C. Janardhana, *Spectrochim. Acta, Part A*, 2008, **69**, 282–285.
31 M. M. Karim, S. H. Lee, Y. S. Kim, H. S. Bae and S. B. Hong, *J. Fluoresc.*, 2006, **16**, 17–22.
32 V. K. Gupta, A. K. Singh and L. K. Kumawat, *Sens. Actuators, B*, 2014, **195**, 98–108.
33 A. Jeanson and V. Béreau, *Inorg. Chem. Commun.*, 2006, **9**, 13–17.
34 Y. S. Kim, G. J. Park, J. J. Lee, S. Y. Lee, S. Y. Lee and C. Kim, *RSC Adv.*, 2015, **5**, 11229–11239.
35 K. Ono and K. Saito, *Heterocycles*, 2008, **75**, 2381–2413.
36 P. Kulkarni, S. Padhye and E. Sinn, *Inorg. Chem. Commun.*, 2003, **6**, 1129–1132.
37 G. Li, N. Liu, S. Liu and S. Zhang, *Electrochim. Acta*, 2008, **53**, 2870–2876.
38 G.-J. Li, N. Liu, P.-K. Ouyang and S.-S. Zhang, *Oligonucleotides*, 2008, **18**, 269–276.
39 B. Machura, I. Nawrot and K. Michalik, *Polyhedron*, 2012, **31**, 548–557.
40 Z. Liu, F. Wen and W. Li, *Thin Solid Films*, 2005, **478**, 265–270.
41 K. Ocakoglu, C. Zafer, B. Cetinkaya and S. Icli, *Dyes Pigm.*, 2007, **75**, 385–394.
42 K. Sako, T. Kakehi, S. Nakano, H. Oku, X. F. Shen, T. Iwanaga, M. Yoshikawa, K. Sugahara, S. Toyota and H. Takemura, *Tetrahedron Lett.*, 2014, **55**, 749–752.
43 F. Cheng, N. Tang and X. Yue, *Spectrochim. Acta, Part A*, 2009, **71**, 1944–1951.
44 F. Cheng, Y. Sun, W. Wu and N. Tang, *Inorg. Chem. Commun.*, 2008, **11**, 687–690.
45 Y. Zhao, Z. Lin, S. Ou, C. Duan, H. Liao and Z. Bai, *Inorg. Chem. Commun.*, 2006, **9**, 802–805.
46 H. Li, S. Zhang, C. Gong, J. Wang and F. Wang, *J. Fluoresc.*, 2016, **26**, 1555–1561.
47 S. J. Zhang, H. Li, C. L. Gong, J. Z. Wang, Z. Y. Wu and F. Wang, *Synth. Met.*, 2016, **217**, 37–42.
48 I. Eckhard and L. Summers, *Aust. J. Chem.*, 1973, **26**, 2727–2728.
49 L. Zhang and B. Li, *Inorg. Chim. Acta*, 2009, **362**, 4857–4861.
50 T. Harel, N. Shefer, Y. Hagooly and S. Rozen, *Tetrahedron*, 2010, **66**, 3297–3300.
51 B. Liu, B.-S. Yang, P.-F. Wang, J. Chai, X.-Q. Hu, T. Gao, T.-G. Chen and J.-B. Chao, *Spectrochim. Acta, Part A*, 2016, **168**, 98–103.